JACS
JOURNAL OF THE AMERICAN CHEMICAL SOCIETY

Communication

pubs.acs.org/JACS

Universal Noble Metal Nanoparticle Seeds Realized Through Iterative Reductive Growth and Oxidative Dissolution Reactions

Matthew N. O'Brien,[†,‡] Matthew R. Jones,[‡,§] Keith A. Brown,[†,‡] and Chad A. Mirkin*[,†,‡,§]

[†]Department of Chemistry, [‡]International Institute for Nanotechnology, [§]Department of Materials Science and Engineering, Northwestern University, Evanston, Illinois 60208, United States

Supporting Information

ABSTRACT: Control over nanoparticle shape and size is commonly achieved via a seed-mediated approach, where nanoparticle precursors, or seeds, are hypothesized to act as templates for the heterogeneous nucleation of anisotropic products. Despite the wide variety of shapes that have been produced via this approach, high yield and uniformity have been more difficult to achieve. These shortcomings are attributed to limited structural control and characterization of the initial distribution of seeds. Herein, we report how iterative reductive growth and oxidative dissolution reactions can be used to systematically control seed structural uniformity. Using these reactions, we verify that seed structure dictates anisotropic nanoparticle uniformity and show that iterative seed refinement leads to unprecedented noble metal nanoparticle uniformities and purities for eight different shapes produced from a single seed source. Because of this uniformity, the first nanoparticle optical extinction coefficients for these eight shapes were analytically determined.

The ability to predict and control the final products of any chemical reaction is limited by the uniformity of the starting materials. This guiding principle is deeply engrained in molecular chemistry where structurally well-defined and analytically pure reagents have enabled the wealth of knowledge and synthetic capabilities that chemists, biologists, and materials scientists now enjoy. In contrast, chemistry involving nanoparticles as reactants, or seeds, for the heterogeneous nucleation of noble metal anisotropic nanoparticle products often does not rely on this tenet due to the difficulty in accessing structurally well-defined particle precursors. Instead, most researchers focus on how to transform an ill-defined initial state into a well-defined end state through manipulation of reaction conditions.[1−4] While this focus on reaction conditions (e.g., reaction rate, the presence of trace metals, ligand affinity) has enabled predictable control of nanoparticle shape, the yield and uniformity of each shape are often not well controlled or understood. Drawing inspiration from molecular chemistry, we hypothesized that a renewed attention to the structural uniformity of the seed precursors could be used to control the yield and uniformity of anisotropic nanoparticle products. However, the inability to prepare a uniform starting point consisting of seeds with a single size, shape, and crystalline defect structure, and to deliberately change seed uniformity and type,[5−9] has precluded rigorous mechanistic studies correlating seed structure with product structure and generalizable methods that consistently produce uniform nanoparticles. Herein, we report how iterative reductive growth and subsequent oxidative dissolution can be used for the stepwise refinement of gold nanoparticle seeds used for anisotropic particle synthesis (Scheme 1). This novel capability allows one to systematically study how size dispersity, shape variation, and crystalline structure of the seed influence anisotropic nanoparticle products and enables the synthesis of eight classes of single crystalline nanostructures from the same batch of seeds, each consisting of a different shape, where the shape and size uniformity exceeds that of all previously reported syntheses.

Scheme 1. (a) An Iterative and Cyclical Process of Reductive Growth and Oxidative Dissolution Was Used To Refine Nanoparticles (red) To Use As Seeds for the Synthesis of Anisotropic Nanoparticle Products (blue). (b) Controlled Oxidative Dissolution of an Anisotropic Nanoparticle with a Au^{3+} Species Occurs Preferentially at Coordinatively Unsaturated Atoms, Wherein Two Au Atoms Are Liberated for Every Au^{3+}

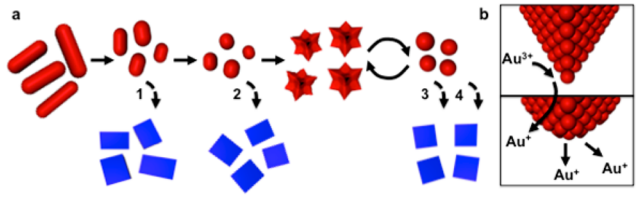

[a]Single crystalline gold nanorods were transformed through oxidative dissolution into pseudo-spherical seeds, reductive growth into concave rhombic dodecahedra, and subsequent oxidative dissolution into spherical seeds. The latter two steps were repeated in a cyclical fashion. Numbers indicate steps where nanoparticles were used as seeds to template the growth of cubes. 4 represents an additional round of the cyclic refinement.

While oxidative dissolution has been used to alter nanoparticle shape through preferential removal of coordinatively unsaturated features on anisotropic nanoparticles,[10−14] cyclical approaches are rarely used in nanoparticle syntheses and in the refinement of a given class of nanostructures. We hypothesized that an iterative process of reductive growth into anisotropic nanostructures and subsequent preferential oxidative dissolu-

Received: April 8, 2014
Published: May 15, 2014

   dx.doi.org/10.1021/ja503509k | J. Am. Chem. Soc. 2014, 136, 7603−7606

tion could be used to refine the size distribution for a batch of nanoparticles to use as more uniform seeds (Scheme 1a). In order to study this, we synthesized seeds from single crystalline gold nanorods, grown via the method pioneered by El-Sayed.[15,16] These structures were chosen because they can be made in greater than 95% yield, which ensures a consistent crystalline structure in the seeds throughout the refinement process (SI Figure S1).[12] When nanorods are exposed to $HAuCl_4$ in the presence of cetyltrimethylammonium bromide, nanorod dissolution proceeds via a conproportionation reaction and occurs preferentially at the more coordinatively unsaturated features at the tips of the rod until a sphere-like geometry is observed, as first reported by Liz-Marzán and co-workers (SI Figure S2a–d).[10] However, after this etching process, the spherical seeds are still disperse in size, with some residual aspect ratio (Figure 1a). Therefore, a reductive growth step was

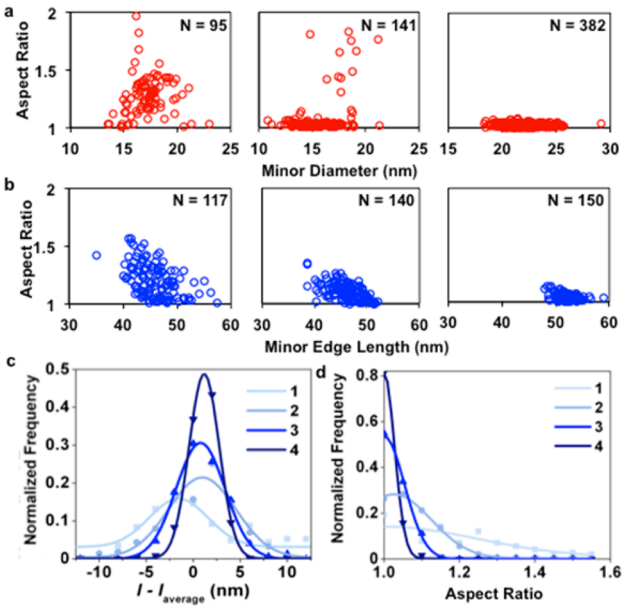

Figure 1. Structural analysis of (a) nanoparticle seeds and (b) cubes grown from these seeds at stages 1, 2, and 3 in the refinement process depicted in Scheme 1 (from left to right, respectively). The number of nanoparticles measured is displayed in the top right of each panel. Frequency plots of (c) the deviation of measured edge length (l) from the average edge length of each sample ($l_{average}$) and (d) aspect ratio are plotted for cubes from 4 subsequent rounds of refinement.

employed to grow seeds into symmetric, highly faceted concave rhombic dodecahedra. During this process, the size distribution further narrows, which we attribute to the dependence of growth rate on the size, radius of curvature, and degree of coordination of the surface atoms of the seed. Reductive growth was followed by a second round of oxidative dissolution, where high-energy sites were again preferentially oxidized (Scheme 1b; Figure 1a) and residual aspect ratio was further removed (SI Figure S3). Importantly, we find that this two-step refinement process can be repeated again to further improve the uniformity of the seeds (Figure 1c, SI Figure S4).

The particles obtained at each step in the refinement process described above can be used to systematically investigate the relationship between seed structural uniformity and anisotropic nanoparticle uniformity in seed-mediated syntheses (Scheme 1a; Figure 1a–d). While this relationship is generally appreciated for the synthesis of core–shell nanoparticles,[17−19] where the relationship between seed and product can be correlated simultaneously, it is more difficult to determine the fate of the seed for single composition aqueous seed-mediated syntheses. The uniformity of a nanoparticle synthesis can be defined by how much a collection of nanostructures deviates from an idealized geometric solid in three important ways: yield, shape, and size. In brief, yield provides information about the selectivity of the synthesis for a particular shape (and is intimately related to the crystalline structure of the seed), while aspect ratio (AR) and coefficient of variation (CV) describe the size and shape uniformity within that given shape (which derive from the physical dimensions of the seed; SI Section VII). Cubes were chosen as the product for this study, as they dry in one orientation ({100}-facets parallel to the surface) with no particle overlap. This is a property that enables an automated and standardized measurement of two dimensions per nanoparticle in a high-throughput fashion (SI Section IV, Figures S7–S9). Analysis of these data revealed that as the size dispersity of the seeds decreased with each step in the refinement process from 21.5% to 15.7% to 7.3% to 4.9% (Figure 1a; SI Figure S4), cubes grown from each set of seeds exhibit the same trend, going from 13.2% to 9.3% to 4.8% to 2.8% (Figure 1b,c; Figure 5), all with yields of >95%. Additional analysis of cube aspect ratio suggests that this improvement in size uniformity extends from both a tightening of absolute dimensions, as well as a narrowing in the distribution of aspect ratios, rather than just a shift in aspect ratio, which remains centered at 1 for all samples (Figure 1d). These trends demonstrate a strong correlation between the uniformity of the seed and the uniformity of the nanoparticle and enable the most uniform synthesis of cubes reported to date.[12,20−24] The change in particle quality can be corroborated through an ensemble measurement of the full width at half-maximum (fwhm) of the localized surface plasmon resonance (LSPR), where inhomogeneities manifest as peak broadening (SI Figure S6).[25,26] Indeed, these data show the fwhm of the seed and cube LSPRs decrease with each refinement step (from 90 to 72 to 60 to 58 nm for seeds and from 86 to 66 to 56 to 55 nm for cubes).

The fundamental hypothesis of our work is that the shape, size, and crystalline structure of the seeds should dictate the uniformity and shape yield of anisotropic nanoparticle products. This simple idea suggests that highly uniform nanoparticle seeds could be used interchangeably in a variety of syntheses as a universal precursor. If true, this would eliminate the need for unique seed synthesis protocols as currently exists in the literature and facilitate a systematic approach to investigation of nanoparticle shape-based phenomena. To confirm this, we used one set of seeds to template the growth of eight unique shapes: cubes, tetrahexahedra,[27] concave cubes,[28] octahedra, cuboctahedra, rhombic dodecahedra,[29] concave rhombic dodecahedra, and truncated ditetragonal prisms[22,30] (Figure 2; SI Figures S12–S24). Importantly, all follow the relationship established above between seed quality and nanoparticle quality and are obtained in greater yield (>95%) with better uniformity than existing reports over a wide range of sizes. The range of shapes generated spans multiple exposed crystal facets ({111}, {110}, {100}, {310}, {520}, {720}), a range of degrees of anisotropy, and includes both concave and convex polyhedra. This property of interchangeability represents the greatest number of shapes generated from a single set of seeds and suggests that the wealth of literature on shape control in seed-mediated nanoparticle synthesis could be

dx.doi.org/10.1021/ja503509k | J. Am. Chem. Soc. 2014, 136, 7603−7606

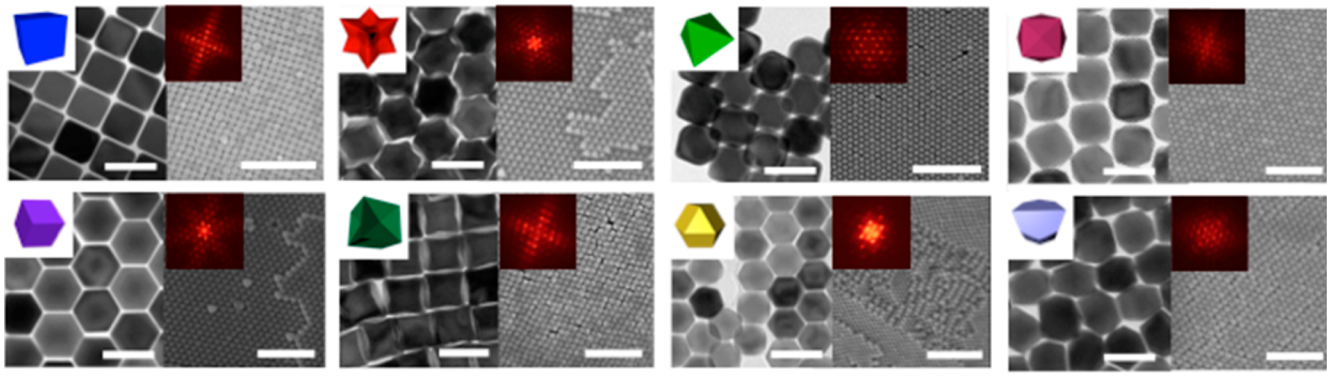

Figure 2. High quality seeds can be used interchangeably to generate eight different shapes. Each panel represents a different shape synthesized from seeds at stage 3 in Scheme 1 and is arranged counterclockwise from top left as three-dimensional graphic rendering of the shape; TEM image (scale bars are 100 nm); high-magnification SEM image of crystallized nanoparticles (scale bars are 500 nm) with FFT pattern inset. Moving clockwise from the top left, the shapes described are cubes, concave rhombic dodecahedra, octahedra, tetrahexahedra, truncated ditetragonal prisms, cuboctahedra, concave cubes, and concave rhombic dodecahedra.

repeated with a renewed focus on seed uniformity to receive markedly better results.

Many fundamental physical and chemical properties of anisotropic nanoparticles have not been experimentally measured due to the lack of sufficiently uniform solutions to correlate bulk behavior with that of individual nanoparticles. One important example of this is an optical extinction coefficient, a property that is influenced by nanoparticle size, shape, and composition and enables one to determine the number of species in a solution with a simple bulk spectroscopic measurement. However, for all gold anisotropic nanoparticle shapes except triangular prisms[31] and rods,[32−34] extinction coefficients have not been determined. To probe the effect of size dispersity on the observed extinction coefficient, we systematically prepared several solutions of cubes with the same average edge length but varied dispersity though the above refinement procedure. Importantly, we found that the extinction coefficients measured for these samples monotonically increases by 40% as the CV decreases from 14.4% to 2.8% (SI Figures S10−S11; Table S1; sections V and VI), showing the importance of size and shape dispersity in determining bulk optical properties. As a result, we have measured extinction coefficients for eight shapes produced from refined seeds, all as a function of size (Table 1). These values enhance our ability to understand trends in optical properties as a function of size, shape, and degree of anisotropy, and simultaneously facilitate the use of these anisotropic nanoparticles.

The seed-focused approach to anisotropic nanoparticle synthesis presented here will help establish a paradigm shift in the field of nanoparticle chemistry toward an emphasis on control and characterization of the starting reagents in order to achieve high quality products. Such an approach likely can be extended to other crystal defect structures (e.g., planar-twinned and penta-twinned seeds) and compositions to not only improve the uniformity of existing nanostructures but also to realize novel morphologies. Furthermore, the systematic approach used to vary particle shape and dispersity make this approach an ideal platform to investigate how nanoparticle uniformity and morphology impact properties and performance in a wide range of applications beyond the extinction coefficient measurements explored here.

Table 1. Average Edge Lengths (l), Dispersity in Edge Length Measured by the Coefficient of Variation (CV), Localized Surface Plasmon Resonance (LSPR), and Extinction Coefficients at the LSPR for Several Sizes of Each Shape Investigated[a]

shape	l (nm)	CV (%)	LSPR (nm)	extinction coefficient (M^{-1} cm^{-1})
cube	43	4.1	538	$4.51 \pm 0.02 \times 10^{10}$
	62	4.0	565	$1.40 \pm 0.01 \times 10^{11}$
	74	4.7	589	$2.17 \pm 0.01 \times 10^{11}$
	87	4.5	602	$2.86 \pm 0.01 \times 10^{11}$
rhombic dodecahedron	39	3.9	556	$8.99 \pm 0.02 \times 10^{10}$
	49	2.4	568	$1.60 \pm 0.01 \times 10^{11}$
	54	3.2	580	$1.87 \pm 0.01 \times 10^{11}$
truncated ditetragonal prism	58	5.4	554	$8.96 \pm 0.03 \times 10^{10}$
	76	4.2	567	$1.64 \pm 0.01 \times 10^{11}$
	99	4.6	583	$3.17 \pm 0.01 \times 10^{11}$
cuboctahedron	40	3.8	531	$2.26 \pm 0.07 \times 10^{10}$
	67	3.3	553	$1.19 \pm 0.01 \times 10^{11}$
concave cube	43	5.6	576	$6.40 \pm 0.01 \times 10^{10}$
	63	6.6	612	$1.54 \pm 0.01 \times 10^{11}$
	84	5.3	648	$2.62 \pm 0.01 \times 10^{11}$
tetrahexahedron	43	3.8	546	$6.95 \pm 0.33 \times 10^{10}$
	62	3.0	572	$1.12 \pm 0.02 \times 10^{11}$
	75	4.0	588	$2.17 \pm 0.02 \times 10^{11}$
octahedron	62	3.7	571	$7.59 \pm 0.01 \times 10^{10}$
	80	2.6	591	$1.43 \pm 0.01 \times 10^{11}$
	110	3.2	624	$2.43 \pm 0.01 \times 10^{11}$
concave rhombic dodecahedron	28	4.2	558	$3.69 \pm 0.02 \times 10^{10}$
	39	3.7	578	$9.56 \pm 0.08 \times 10^{10}$
	56	2.4	608	$2.50 \pm 0.01 \times 10^{11}$

[a]Nanoparticle dimensions were measured from at least 100 nanoparticles for each sample, details of which can be found in the Supporting Information (SI Section VII; Figures S13−S24).

dx.doi.org/10.1021/ja503509k | J. Am. Chem. Soc. 2014, 136, 7603−7606

■ ASSOCIATED CONTENT

Supporting Information

Experimental details and additional data. This material is available free of charge via the Internet at http://pubs.acs.org.

■ AUTHOR INFORMATION

Corresponding Author

*Email: chadnano@northwestern.edu.

Notes

The authors declare no competing financial interest.

■ ACKNOWLEDGMENTS

This material is based upon work supported by the AFOSR under Award Nos. FA9550-09-1-0294 and FA9550-11-1-0275; the Nonequilibrium Energy Research Center (NERC), an Energy Frontier Research Center funded by the U.S. Department of Energy, Office of Science, Office of Basic Energy Sciences under Award Number DE-SC0000989; and the National Science Foundation's MRSEC program (DMR-1121262) at the Materials Research Center of Northwestern University. M.N.O. is grateful to the NSF for a Graduate Research Fellowship. M.R.J. is grateful to the NSF for a Graduate Research Fellowship and to Northwestern University for a Ryan Fellowship. K.A.B. gratefully acknowledges support from Northwestern University's International Institute for Nanotechnology. This work made use of the EPIC facility (NUANCE Center-Northwestern University), which has received support from the MRSEC program (NSF DMR-1121262) at the Materials Research Center, and the Nanoscale Science and Engineering Center (EEC-0118025/003), both programs of the National Science Foundation; the State of Illinois; and Northwestern University. Inductively coupled plasma atomic emission spectroscopy was performed at the Integrated Molecular Structure Research and Education Center (IMSERC) at Northwestern University. We thank Prof. George Schatz for helpful discussions.

■ REFERENCES

(1) Tao, A. R.; Habas, S.; Yang, P. D. *Small* **2008**, *4*, 310.
(2) Xia, Y. N.; Xiong, Y. J.; Lim, B.; Skrabalak, S. E. *Angew. Chem. Int. Ed.* **2009**, *48*, 60.
(3) Personick, M. L.; Mirkin, C. A. *J. Am. Chem. Soc.* **2013**, *135*, 18238.
(4) Lohse, S. E.; Burrows, N. D.; Scarabelli, L.; Liz-Marzán, L. M.; Murphy, C. J. *Chem. Mater.* **2014**, *26*, 34.
(5) Lofton, C.; Sigmund, W. *Adv. Funct Mater.* **2005**, *15*, 1197.
(6) Elechiguerra, J. L.; Reyes-Gasga, J.; Yacaman, M. J. *J. Mater. Chem.* **2006**, *16*, 3906.
(7) Langille, M. R.; Zhang, J.; Personick, M. L.; Li, S.; Mirkin, C. A. *Science* **2012**, *337*, 954.
(8) Brown, K. R.; Walter, D. G.; Natan, M. J. *Chem. Mater.* **2000**, *12*, 306.
(9) Gole, A.; Murphy, C. J. *Chem. Mater.* **2004**, *16*, 3633.
(10) Rodriguez-Fernandez, J.; Perez-Juste, J.; Mulvaney, P.; Liz-Marzan, L. M. *J. Phys. Chem. B* **2005**, *109*, 14257.
(11) Tsung, C. K.; Kou, X. S.; Shi, Q. H.; Zhang, J. P.; Yeung, M. H.; Wang, J. F.; Stucky, G. D. *J. Am. Chem. Soc.* **2006**, *128*, 5352.
(12) Niu, W. X.; Zheng, S. L.; Wang, D. W.; Liu, X. Q.; Li, H. J.; Han, S. A.; Chen, J.; Tang, Z. Y.; Xu, G. B. *J. Am. Chem. Soc.* **2009**, *131*, 697.
(13) Hong, S.; Shuford, K. L.; Park, S. *Chem. Mater.* **2011**, *23*, 2011.
(14) Lee, Y.-J.; Schade, N. B.; Sun, L.; Fan, J. A.; Bae, D. R.; Mariscal, M. M.; Lee, G.; Capasso, F.; Sacanna, S.; Manoharan, V. N.; Yi, G.-R. *ACS Nano* **2013**, *7*, 11064.
(15) Nikoobakht, B.; El-Sayed, M. A. *Chem. Mater.* **2003**, *15*, 1957.
(16) Liu; Guyot-Sionnest, P. *J. Phys. Chem. B* **2005**, *109*, 22192.
(17) Murray, C. B.; Norris, D. J.; Bawendi, M. G. *J. Am. Chem. Soc.* **1993**, *115*, 8706.
(18) Dabbousi, B. O.; RodriguezViejo, J.; Mikulec, F. V.; Heine, J. R.; Mattoussi, H.; Ober, R.; Jensen, K. F.; Bawendi, M. G. *J. Phys. Chem. B* **1997**, *101*, 9463.
(19) Ghosh Chaudhuri, R.; Paria, S. *Chem. Rev.* **2012**, *112*, 2373.
(20) Sau, T. K.; Murphy, C. J. *J. Am. Chem. Soc.* **2004**, *126*, 8648.
(21) Seo, D.; Park, J. C.; Song, H. *J. Am. Chem. Soc.* **2006**, *128*, 14863.
(22) Langille, M. R.; Personick, M. L.; Zhang, J.; Mirkin, C. A. *J. Am. Chem. Soc.* **2012**, *134*, 14542.
(23) Sohn, K.; Kim, F.; Pradel, K. C.; Wu, J. S.; Peng, Y.; Zhou, F. M.; Huang, J. X. *ACS Nano* **2009**, *3*, 2191.
(24) Wu, H. L.; Kuo, C. H.; Huang, M. H. *Langmuir* **2010**, *26*, 12307.
(25) Link, S.; El-Sayed, M. A. *J. Phys. Chem. B* **1999**, *103*, 8410.
(26) Link, S.; El-Sayed, M. A. *J. Phys. Chem. B* **1999**, *103*, 4212.
(27) Ming, T.; Feng, W.; Tang, Q.; Wang, F.; Sun, L.; Wang, J.; Yan, C. *J. Am. Chem. Soc.* **2009**, *131*, 16350.
(28) Zhang, J. A.; Langille, M. R.; Personick, M. L.; Zhang, K.; Li, S. Y.; Mirkin, C. A. *J. Am. Chem. Soc.* **2010**, *132*, 14012.
(29) Personick, M. L.; Langille, M. R.; Zhang, J.; Mirkin, C. A. *Nano Lett.* **2011**, *11*, 3394.
(30) Lu, F.; Zhang, Y.; Zhang, L. H.; Zhang, Y. G.; Wang, J. X.; Adzic, R. R.; Stach, E. A.; Gang, O. *J. Am. Chem. Soc.* **2011**, *133*, 18074.
(31) Jones, M. R.; Mirkin, C. A. *Angew. Chem., Int. Ed.* **2013**, *52*, 2886.
(32) Liao, H.; Hafner, J. H. *Chem. Mater.* **2005**, *17*, 4636.
(33) Orendorff, C. J.; Murphy, C. J. *J. Phys. Chem. B* **2006**, *110*, 3990.
(34) Near, R. D.; Hayden, S. C.; Hunter, R. E.; Thackston, D.; El-Sayed, M. A. *J. Phys. Chem. C* **2013**, *117*, 23950.

■ NOTE ADDED AFTER ASAP PUBLICATION

After this paper was published ASAP May 15, 2014, a correction was made to the grouping of the data in Table 1. The corrected version was reposted May 16, 2014.